MCB
Journals.ASM.org

DNMT1 Is Regulated by ATP-Citrate Lyase and Maintains Methylation Patterns during Adipocyte Differentiation

Tatiana Londoño Gentile,[a]* Chao Lu,[a,b]* Peter M. Lodato,[a] Sarah Tse,[a] Scott H. Olejniczak,[b] Eric S. Witze,[a] Craig B. Thompson,[b] Kathryn E. Wellen[a]

Department of Cancer Biology, Abramson Family Cancer Research Institute, Perelman School of Medicine, University of Pennsylvania, Philadelphia, Pennsylvania, USA[a]; Cancer Biology and Genetics Program, Memorial Sloan-Kettering Cancer Center, New York, New York, USA[b]

During adipocyte differentiation, significant epigenomic changes occur in association with the implementation of the adipogenic program. We have previously shown that histone acetylation increases during differentiation in a manner dependent on acetyl coenzyme A (acetyl-CoA) production by the enzyme ATP-citrate lyase (ACL). Whether ACL regulates nuclear targets in addition to histones during differentiation is not clear. In this study, we report that DNA methyltransferase 1 (DNMT1) levels in adipocytes are controlled in part by ACL and that silencing of DNMT1 can accelerate adipocyte differentiation. DNMT1 gene expression is induced early in 3T3-L1 adipocyte differentiation during mitotic clonal expansion and is critical for maintenance of DNA and histone H3K9 methylation patterns during this period. In the absence of DNMT1, adipocyte-specific gene expression and lipid accumulation occur precociously. Later in differentiation, DNMT1 levels decline in an ACL-dependent manner. ACL-mediated suppression of DNMT1 occurs at least in part by promoting expression of microRNA 148a (miR-148a), which represses DNMT1. Ectopic expression of miR-148a accelerates differentiation under standard conditions and can partially rescue a hypermethylation-mediated differentiation block. The data suggest a role for DNMT1 in modulating the timing of differentiation and describe a novel ACL-miR-148a-dependent mechanism for regulating DNMT1 during adipogenesis.

The process of adipocyte differentiation occurs upon the activation of a well-characterized transcriptional program that enables precursor cells to take on the characteristics of differentiated adipocytes, including the ability to take up glucose in an insulin-responsive manner and store triglyceride in lipid droplets (1–3). The transcription factor peroxisome proliferator-activated receptor gamma (PPARγ) is considered the master regulator of adipogenesis, and CCAAT/enhancer-binding proteins (CEBPα, -β, and -δ) also play key roles in this process. The differentiation process is associated with broad changes in the epigenome, as characterized in recent chromatin immunoprecipitation-sequencing (ChIP-Seq) studies (4, 5). Activating marks, including H3K9ac, H3K27ac, and H3K4me2/3, increase at promoters and enhancers of genes that are induced during adipocyte differentiation (4, 5). Chromatin remodeling is initiated within the first few hours of the differentiation process, with recruitment of multiple transcription factors to key "hot spots" (6). Additionally, an epigenomic transition state has been characterized at sites bound by the glucocorticoid receptor (GR) and CEBPβ, which display transient increases in histone acetylation at early time points in adipogenesis (5).

Epigenomic changes during adipocyte differentiation are also reflected in global levels of histone marks. In previous work, we showed that levels of histone H3 and H4 acetylation in 3T3-L1 adipocytes increase during differentiation and are regulated in a manner dependent on glucose availability (7). This nutrient-dependent acetylation requires the enzyme ATP-citrate lyase (ACL), which generates acetyl coenzyme A (acetyl-CoA) through the cleavage of citrate. ACL is present in both the cytoplasm and the nucleus, suggesting that acetyl-CoA is produced in both of these compartments by this enzyme and implying that nuclear production of acetyl-CoA might be important for the regulation of nuclear acetylation events (7). Increased histone acetylation during differentiation occurs in parallel with decreased levels of repressive histone H3K9 di- and trimethylation marks (8). Silencing of the H3K9 demethylase KDM4C impairs adipogenesis, indicating that downregulation of this mark is important for differentiation (8).

Coordination of activating and repressive histone modifications during adipocyte differentiation could potentially occur passively; for example, increases in acetylation could dilute out the effects of methyltransferases acting on the same lysine residues. On the other hand, it is possible that mechanisms exist to actively coordinate these marks. Several acetyl-proteomics studies have recently been published, which have revealed acetylation to be an extremely prevalent modification in cells, with thousands of cellular proteins acetylated (9–12). Among these, a central theme emerging from these studies is that many mitochondrial and cytoplasmic metabolic enzymes are acetylated (13). At least several of these enzymes are acetylated in a nutrient-responsive manner, and acetylation may play a key role in fine-tuning metabolic regulation (13). For example, the gluconeogenic enzyme phosphoenolpyruvate carboxykinase (PEPCK) is acetylated in a glucose-responsive manner, promoting its ubiquitination and proteosomal degradation; thus, under high-glucose conditions,

Received 7 November 2012 **Returned for modification** 28 November 2012
Accepted 19 July 2013
Published ahead of print 29 July 2013
Address correspondence to Kathryn E. Wellen, wellenk@exchange.upenn.edu.
* Present address: Tatiana Londoño Gentile, Robert Wood Johnson Medical School, Piscataway, New Jersey, USA; Chao Lu, Laboratory of Chromatin Biology and Epigenetics, The Rockefeller University, New York, New York, USA.
C.L. and P.M.L. contributed equally to this article.

doi:10.1128/MCB.01495-12

gluconeogenesis might be suppressed in part through increased degradation of PEPCK (14). In addition to metabolic enzymes, numerous chromatin-modifying enzymes were also found to be acetyl-proteins (9, 10). We therefore hypothesized that ACL has a role in epigenetic regulation beyond histone acetylation, through the regulation of other types of chromatin-regulatory proteins.

The DNA methyltransferase 1 (DNMT1) has been shown to be acetylated on at least 16 lysines (10, 15, 16), and acetylation has been implicated in targeting DNMT1 for degradation (15). DNA methylation can occur either *de novo* or as a maintenance function to maintain methylation patterns on daughter DNA strands during replication. DNMT3a and DNMT3b function predominantly in *de novo* DNA methylation, whereas DNMT1 is thought to be the main maintenance methyltransferase (17, 18). In this study, we examined a potential role for ACL in the regulation of DNMT1. Although DNA methylation has been well studied in other contexts, such as cancer (19, 20), its role in the regulation of adipogenesis is poorly understood. In classic studies, Taylor and Jones showed that short-term treatment of C3H10T1/2 or 3T3 cells with DNMT inhibitors such as 5-azacytidine triggered spontaneous differentiation to multiple phenotypes, including adipocyte, that emerged several weeks later (21). On the other hand, treatment of 3T3-L1 preadipocytes with DNMT inhibitors for 2 days prior to induction of differentiation impaired the cells' capacity to differentiate, suggesting that DNA methylation may be important for licensing preadipocytes for adipogenesis (22). The roles of DNA methylation and DNA methyltransferases after the induction of adipogenesis remain to be elucidated.

Upon induction of differentiation in 3T3-L1 adipocytes, cells undergo two synchronous rounds of cell division, termed mitotic clonal expansion (MCE), after which they undergo growth arrest followed by terminal differentiation (3). We hypothesized that DNMT1 might be important for maintaining patterns of DNA methylation during MCE and explored a role for ACL in the regulation of DNMT1 during adipocyte differentiation. We show here that DNMT1 plays a key role in regulating histone and DNA methylation during early adipocyte differentiation, that silencing of DNMT1 accelerates differentiation, and that ACL suppresses DNMT1 protein levels later in differentiation. Surprisingly, we failed to detect a difference in DNMT1 acetylation upon silencing of ACL. Instead, we found that ACL can suppress DNMT1 by promoting the expression of microRNA 148a (miR-148a), a microRNA known to target DNMT1. Ectopic expression of miR-148a recapitulates the early differentiation phenotype observed upon silencing of DNMT1 and can partially reverse a hypermethylation-mediated differentiation block. Overall, the results show that DNMT1 plays a role in maintaining DNA methylation patterns during early adipogenesis and that DNMT1 is suppressed later in adipogenesis in part through an ACL-miR-148a-dependent mechanism.

MATERIALS AND METHODS

Cell culture and transfections. 3T3-L1 cells and C3H10T1/2 cells were maintained in Dulbecco modified Eagle medium (DMEM) with 10% fetal bovine serum (FBS). Stable cell lines expressing IDH mutants have been previously described (8). Small interfering RNA (siRNA) transfections were performed with Lipofectamine RNAiMAX (Invitrogen), using siRNA pools targeting murine ACL (Dharmacon L-040092-01), murine DNMT1 (Dharmacon L-056796-01), or a nontargeting control (Dharmacon D-001810-01-20) at a final concentration of 20 nM. Ectopic expression of microRNAs was performed with Lipofectamine RNAiMAX using pre-miR miRNA precursor molecules of hsa-miR-148 (Ambion AM17100) and negative control 1 (Ambion AM17110) at a final concentration of 1 nM. The 1 nM concentration was selected for experiments after titration of miR-148a to achieve expression close to that observed in differentiated adipocytes (data not shown). Locked nucleic acid (LNA) microRNA inhibitors (control and miR-148a inhibitors) were used at 50 nM. Transfections for each of these reagents (siRNAs, microRNAs, or microRNA inhibitors) were performed 3 days prior to inducing differentiation. The ACL inhibitor 3,3,14,14-tetramethylhexadecanedioic acid (Medica 16; Sigma M5693) was used at the indicated doses.

Differentiation of 3T3-L1 and C3H10T1/2 adipocytes. Differentiation of 3T3-L1 and C3H10T1/2 adipocytes was conducted according to a standard protocol, as previously described (7). Briefly, at 2 days postconfluence, cells were stimulated for 2 days with a cocktail containing 0.5 mM isobutylmethylxanthine, 1 μM dexamethasone, 5 μg/ml insulin, and 5 μM troglitazone (all from Sigma) in DMEM with 10% FBS. After 2 days, cells were placed into medium containing 10% FBS and insulin, and the medium was replaced every 2 days after that. Differentiation was performed in DMEM containing 25 mM glucose, except in experiments with variable glucose concentrations, in which case glucose-free DMEM (Invitrogen) was used and supplemented with the indicated amounts of D-glucose (Sigma). Dialyzed FBS was used for all experiments performed with specific glucose concentrations. Acetate complementation was performed using sodium acetate (NaOAc) (pH 7.0) at a final concentration of 5 mM. For all differentiation experiments using siRNA, preadipocytes were transfected 3 days prior to induction of differentiation.

Lipid staining. Lipid accumulation was evaluated using Bodipy 493/503 (Invitrogen). A 20-μg/ml concentration of dye in phosphate-buffered saline (PBS) was loaded into cells by incubating for 45 min at 37°C. Cells were washed and allowed to recover for 60 min in full medium. Live cells were imaged using an Olympus IX81 fluorescence inverted microscope (see Fig. 3) or a Leica AF6000 inverted microscope (see Fig. 6). Oil Red O lipid staining was performed on day 6 adipocytes, as previously described (7). Briefly, cells were washed and then fixed for 20 min at room temperature in 3% paraformaldehyde. Cells were washed with distilled water (dH_2O) and then stained with Oil Red O solution. For quantification, Oil Red O was dissolved in isopropanol and absorbance measured at 500 nm.

Live-cell imaging. Live-cell imaging was performed on a Leica AF6000 inverted microscope at 37°C under 5% CO_2. Cells were imaged on Matek dishes using a 10× objective. Images were collected every 10 min on a Hamamatsu ORCA-R2 camera. Quantitation was performed manually by counting the numbers of dividing cells and numbers of lipid droplet-containing cells in six different frames.

Cell count assays and metabolite measurements. Cell counts were carried out in triplicate in 12-well dishes using the Countess automated cell counter (Invitrogen) and the Countess cell counting chamber slides with trypan blue (Invitrogen, C10228). 3T3-L1 preadipocytes were transfected with control or DNMT1-targeting siRNA as described above and 2 days later were induced to differentiate into adipocytes. At 0 and 96 h, cell counts were carried out. Cells were gently washed with PBS, trypsinized, resuspended in 1 ml of medium, and transferred to Eppendorf tubes. Cells were then vortexed, 10-μl aliquots for each sample were placed in fresh tubes with 10 μl of trypan blue (Invitrogen), and 10-μl aliquots were loaded into both sides of the cell counting chamber slides. Each sample was read in duplicate. From these same samples, medium metabolite levels were measured. Medium was collected from cells at day 2 and day 4, and glucose consumption was measured using a YSI 7100 Analyzer. Total glucose consumption and lactate production were summed over the 2 days and subtracted from values for a medium-only control that was incubated for the same amount of time at 37°C. Metabolite consumption or production was calculated as previously described (23). Briefly, metabolite consumption was defined as $v = V(x_{\text{medium control}} - x_{\text{final}})/A$, where v is metabolite consumption/production, V is culture volume, x is metabolite concentration, and A is cell number area under the curve. A was calculated as $N(T)d/\ln 2(1 - 2^{-T/d})$, where $N(T)$ is final cell count, d is

doubling time, and T is time of experiment. Doubling time was calculated as $d = (T)[\log(2)/\log(Q2/Q1)]$, where $Q1$ is starting cell number and $Q2$ is final cell number.

Immunoblotting. Total protein extracts were harvested for analysis, at the indicated time points, by lysis with radioimmunoprecipitation assay (RIPA) buffer (1% NP-40, 0.5% deoxycholate, 0.1% SDS, 150 mM NaCl, 50 mM Tris [pH 8], with added protease inhibitors), followed by brief sonication. Sodium butyrate (5 mM) was included in buffer for samples in which acetylation was assessed. For DNMT1 protein assessment, samples were subjected to longer sonication using a Branson Sonifier 250 for a total of 10 s in increments of 3 s, 3 s, and 4 s at a constant output of 3.5 while on ice. Protein concentrations were quantified by bicinchoninic acid (BCA) protein assay (Pierce), and samples were run on NuPage gels (Invitrogen) for Western blotting. The following antibodies were used: acetyl lysine (Immunechem), AcH3 (Millipore, 06-599), AcH4 (Millipore, 06-866), ACL (described previously [24]), CEBPβ (Santa Cruz, sc-150), H3K9me3 (Abcam, ab8898), DNMT1 (Active Motif, 39905), myc tag (Cell Signaling, 2278), PPARγ (Santa Cruz, sc-7196), histone H3 (Millipore, 06-755), histone H4 (Millipore, 04-858), and tubulin (Sigma, T6199) antibodies. Blots were imaged using either film or a LiCor Odyssey infrared imaging system. Blot quantification was performed using ImageJ software.

DNMT1 acetylation analysis. HEK-293T cells were plated to reach 90 to 95% confluence, and pcDNA4-TO-myc-DNMT1 (a kind gift of Zhenghe Wang, Case Western Reserve University) or vector control DNA was transfected into cells, using Lipofectamine 2000 (Invitrogen) as per the manufacturer's instruction. ACL-targeting or control siRNA pools were transfected into cells 1 day prior to myc-DNMT1 transfection. Sodium acetate (5 mM) was added to cells at 24 h after myc-DNMT1 transfection, and cells were harvested after another 24-hour treatment. Cells were lysed in RIPA buffer with added protease inhibitor cocktail (Complete Mini; Roche) and 5 mM sodium butyrate. Samples were sonicated and quantified. A 0.5- to 1-mg quantity of protein was used for overnight immunoprecipitation (IP) using 10 μl of myc tag magnetic bead conjugate (Cell Signaling, 5698). The following day, samples were pelleted by magnetic separation and beads washed for 3 to 5 min on rotating platform at 4°C with RIPA buffer, followed by Tris-EDTA (TE) buffer. Samples were eluted in 2× sample buffer and analyzed by Western blotting.

2-Deoxy[^{14}C]glucose uptake assay. Insulin-stimulated glucose uptake was done as previously described (25), except that 2-deoxy[^{14}C]glucose was used as the tracer. Briefly, cells were starved of serum overnight. Glucose uptake assay was performed in Krebs-Ringer-HEPES (KRH) buffer. Cells were treated in the presence or absence of insulin in KRH buffer for 20 min. Glucose tracer was added and left for an additional 10 min. The reaction was stopped on ice, cells lysed, and lysates subjected to scintillation counting. Counts per minute were normalized to cell number.

Chromatin fractionation. Cells were fractionated into cytoplasmic, nucleoplasmic, and chromatin-associated fractions, essentially as described previously (26). Briefly, cells were lysed in buffer A (10 mM HEPES, 10 mM KCl, 1.5 mM $MgCl_2$, 0.34 M sucrose, 10% glycerol, 1 mM dithiothreitol [DTT], 0.1% Triton X). After incubation on ice and centrifugation, supernatants were collected as the cytoplasmic fraction. Pellets contained nuclei and were lysed in buffer B (3 mM EDTA, 0.2 mM EGTA, 1 mM DTT). After incubation on ice and centrifugation, supernatants were collected as nucleoplasmic fraction. Pellets were resuspended in high-salt buffer (50 mM Tris [pH 8], 0.05% NP-40, 0.45 M NaCl). After incubation on ice and centrifugation, supernatants were collected as the chromatin fraction.

Q-PCR analysis. RNA was isolated from triplicate wells under each condition using TRIzol (Invitrogen) and cDNA synthesized using high-capacity RNA-to-cDNA master mix (Applied Biosystems), as per the kit instructions. A 20-μl reaction mixture was prepared for each sample using 1 μg of RNA, 4 μl of the master mix, and the remaining amount double-distilled water (ddH_2O). For mature microRNA cDNA synthesis we used the TaqMan MicroRNA reverse transcription kit (Applied Biosystems, 4366596), as per the manufacturer's instructions. Quantitative PCR (Q-PCR) was performed on a 7900HT sequence detection system (Applied Biosystems) using TaqMan gene expression assays (Applied Biosystems), including murine DNMT1 (Mm01151063_m1), murine Fabp4 (Mm00445878_m1), murine mmu-miR-103-1 (Mm03306910_pri), murine mmu-miR-148a (Mm03306713_pri), murine P/CAF (Mm00451387_m1), murine Slc2a4 (Glut4) (Mm01245507_g1), murine Tip60 (Mm01231512_m1), murine LDHA (Mm01612132), murine adipsin (Mm00442664), and hsa-miR-148a (Applied Biosystems, 000470), U6 snRNA (Applied Biosystems, 001973), or Sybr assays. The primer sequences used are given in Table 1. Gene expression data were normalized to 18S rRNA or actin, as indicated.

TABLE 1 Primers used for qPCR and ChIP

Procedure	Name	Sequence (5′→3′)
qPCR	Pparg forward	TCGCTGATGCACTGCCTATG
	Pparg reverse	GAGAGGTCCACAGAGCTGATT
	Adiponectin forward	GATGGCAGAGATGGCACTCC
	Adiponectin reverse	CTTGCCAGTGCTGCCGTCAT
	Dnmt3a forward	AGCGTCACACAGAGCATATCCAGGAAG
	Dnmt3a reverse	GGCCAGTACCCTCATAAAGTCCCTTGC
	Dnmt3b forward	ATGGAATTGCAACGGGGTACTTGGTGC
	Dnmt3b reverse	CTGGCCTTCATGCTTAACAGTTCCCAC
	Fasn forward	GGAGGTGGTGATAGCCGGTAT
	Fasn reverse	TGGGTAATCCATAGAGCCCAG
ChIP	miR-148a 0kb forward	GAACCTGCTGACTTGACACG
	miR-148a 0kb reverse	CACTGGAAGCCTAGCTCAGC
	miR-148a −0.5kb forward	GAAACTGGCTTGTGTTCGC
	miR-148a −0.5kb reverse	GCCAAAGTTTAGTAACAGGAACC
	Glut4 0kb forward	CTTATTGCAGCGCCTGAGT
	Glut4 0kb reverse	GGGCTGGCTATTTATATTCAGC
	Glut4 −1kb forward	AGAACCAGTGTAGAGACTATGTGGAG
	Glut4 −1kb reverse	TAGGAACGGAAGTTATTGGTCC
	Glut4 +1kb forward	GAGGTCCAGATCCTCAAACTTT
	Glut4 +1kb reverse	ATATGGCCCACTTTCTCTCATC
	Fabp4 −1.5kb forward	GATTGATGAATTCAAGTTGTTTCA
	Fabp4 −1.5kb reverse	GTAGAGCCAGCCCATGTAAACTT
	Fabp4 0kb forward	TATCTGGACTTCAGAGGCTCAT
	Fabp4 0kb reverse	ACTTCTTTCATGTAATCATCGAAGTT
	Fabp4 +1kb forward	GCCCATCGACTGTTTACTGTTC
	Fabp4 +1kb reverse	GCCTTTAATCATGGGTCTCTCA

ChIP. Chromatin immunoprecipitation (ChIP) was performed with the Millipore Magna ChIP G kit (Millipore, 17-611) or equivalent homemade buffers. Under the indicated conditions, cells were cross-linked with 1% formaldehyde for 10 min at room temperature and then quenched with 10% of 10× glycine. After washing with cold PBS, cells were centrifuged and lysed in 500 μl cell lysis buffer (10 mM Tris [pH 8], 10 mM NaCl, 1.5 mM $MgCl_2$, 0.5% NP-40) for 15 min on ice. Cells were centrifuged, and the nuclear pellet was resuspended in 500 μl of nuclear lysis buffer (50 mM Tris [pH 8], 5 mM EDTA, 1% SDS). The lysate was then sonicated for 30 cycles on high using a Bioruptor sonicator 300 (Diagenode) to shear DNA to approximately 200 to 600 bp. Samples were spun down and supernatant diluted 1:10 in dilution buffer (16.7 mM Tris [pH 8], 1.1% Triton X, 0.01% SDS, 167 mM NaCl, 1.2 mM EDTA) and used for triplicate immunoprecipitations overnight with protein G magnetic beads. Each IP utilized supernatant either from 10^6 cells (AcH4 ChIPs) or 100 μg protein (AcH3K9me2 ChIPs). Primary antibodies used were anti-acetyl-histone H4 antibody (Millipore, 06-866) and dimethyl histone H3 (Lys9) antibody (Cell Signaling, 9753). The next day, samples were washed in low-salt buffer (0.1% SDS, 1% Triton-X, 2 mM EDTA, 20 mM Tris [pH 8], 150 mM NaCl), high-salt buffer (0.1% SDS, 1% Triton-X, 2

mM EDTA, 20 mM Tris [pH 8], 500 mM NaCl), LiCl buffer (1% NP-40, 1% deoxycholate, 1 mM EDTA, 10 mM Tris [pH 8], 250 mM LiCl), and TE buffer (10 mM Tris [pH 8], 1 mM EDTA). Histone complexes were eluted from beads twice at 65 °C for 10 min in elution buffer (10 mM Tris [pH 8], 1 mM EDTA, 1% SDS, 150 mM NaCl, 5 mM DTT), eluates were combined, and cross-links were reversed by incubating eluates for 6 h at 65°C. Proteinase K was added and eluates incubated for 1 h at 45°C. DNA was recovered using Millipore Magna ChIP G kit (Millipore, 17-611) or chromatin IP DNA purification kit (Active Motif, 58002) columns. Quantitative PCR was performed on purified DNA samples. Primer sequences are given in Table 1.

Quantitative DNA methylation analysis. 3T3-L1 preadipocytes were transfected in triplicate with control or DNMT1 siRNA as described above and 2 days later were induced to differentiate into adipocytes. At 0 h, 2 days, and 4 days after induction of differentiation, purification of DNA was carried out using the Qiagen DNeasy blood and tissue kit (69504), as per the manufacturer's instruction. After bisulfite conversion, the methylation percentage at CpG was measured using the MassArray EpiTYPER assay (Sequenom) as previously described (27). Primers were designed to cover CpG islands at gene promoters using Sequenom EpiDesigner software (http://www.epidesigner.com/). Primer sequences and raw data tables are available upon request.

Adipocyte/stromal-vascular fractionation of white adipose tissue. Visceral adipose tissue was dissected from adult female FVB/N mice, weighing 30 to 40 g, kindly provided to us by C. Sterner and L. Chodosh from their colony. Adipose tissue was finely minced with scissors and dissociated by shaking incubation in Liberase TL at 37°C for 45 min (Roche). Digestion was stopped by addition of DMEM plus 10% FBS and cells filtered through 150-μm mesh. The cell suspension was centrifuged for 10 min at 500 relative centrifugal force (RCF). Adipocytes were contained in the top layer and were removed to a fresh tube, washed with PBS, and lysed in RIPA buffer. The stromal-vascular fraction was pelleted at the bottom of the tube. Supernatant was aspirated, and cells were washed in PBS and lysed in RIPA buffer. All samples were sonicated as described above and analyzed by Western blotting. Protocols were approved by the University of Pennsylvania IACUC.

RESULTS

We have previously shown that ACL-dependent production of acetyl-CoA can contribute to the regulation of nuclear histone acetylation (7). Protein levels of a key chromatin-modifying enzyme, DNMT1, were recently shown to be regulated by acetylation (15). To test whether ACL contributes to the regulation of DNMT1, we examined the effects of silencing ACL on DNMT1 during the adipocyte differentiation of 3T3-L1 and C3H10T1/2 cells. DNMT1 levels decreased by 4 days following induction of differentiation, and ACL silencing partially blocked this decrease in both cell lines (Fig. 1A and B). DNMT1 levels were similarly maintained during differentiation when cells were treated with an ACL inhibitor (Fig. 1C). ACL-dependent regulation of DNMT1 occurs at a posttranscriptional level, since DNMT1 mRNA levels were not elevated in the absence of ACL (Fig. 1A). Thus, ACL regulates DNMT1 protein levels during differentiation, suggesting that increased acetyl-CoA production during differentiation might mediate suppression of DNMT1.

To better understand the regulation of DNMT1 during adipocyte differentiation, we monitored DNMT1 mRNA and protein levels over a time course after induction of differentiation in 3T3-L1 cells. DNMT1 mRNA and protein levels increased by 24 h after induction of differentiation and decreased later in differentiation after growth arrest, consistent with a potential role for DNMT1 in maintaining DNA methylation during MCE in 3T3-L1 cells (Fig. 1D and E). DNMT3a and 3b mRNA levels, in contrast, are low during MCE and increase later in differentiation (Fig. 1D). To confirm that these patterns of DNMT1 regulation were reflective of chromatin-associated DNMT1, we fractionated 3T3-L1 cells at days 0, 1, and 6 of differentiation into cytoplasmic, nucleoplasmic, and chromatin-associated fractions. The majority of DNMT1 was present in chromatin, and chromatin-associated DNMT1 increased at day 1 and decreased later in differentiation (Fig. 1F). To assess whether similar regulation of DNMT1 also occurs in adipose tissue *in vivo*, we separated freshly harvested murine white adipose tissue into adipocyte and stromal-vascular fractions and examined DNMT1 levels. Consistent with the *in vitro* data, DNMT1 was present in the preadipocyte-containing stromal-vascular fraction but was almost undetectable in adipocytes (Fig. 1G).

We next sought to determine whether DNMT1 functionally regulates DNA methylation during early adipogenesis. DNMT1 was silenced by transfecting siRNA into preadipocytes 3 days prior to inducing differentiation. Bisulfite conversion and sequencing were performed to examine DNA methylation during differentiation. *Glut4* and *Pparg* are both highly induced during terminal adipocyte differentiation. We examined methylation of 52 CpG dinucleotides within the *Glut4* promoter and of 37 CpGs in the *Pparg* locus at days 0, 2, and 4 after induction of differentiation (Fig. 2A). Methylation of *Glut4* and *Pparg* did not significantly change during the first 4 days of differentiation in control cells; however, upon silencing of DNMT1 and between days 0 and 2, during the MCE period, a pronounced decrease in DNA methylation was observed (Fig. 2A). Specifically, for *Glut4*, CpGs were on average 53% methylated at day 0 in control cells and this remained unchanged to day 4. In siDNMT1 cells, CpGs were on average 45% methylated at day 0, 33% at day 2, and 32% at day 4. For *Pparg*, CpGs assessed were on average 80% methylated at day 0 in control cells and 78% methylated at days 2 and 4. In siDNMT1 cells, CpGs were on average 75% methylated at day 0, 55% at day 2, and 53% at day 4. These data indicate that DNMT1 is critical for maintaining DNA methylation patterns during early adipogenesis.

In addition to regulating DNA methylation, DNMT1 performs scaffolding functions. The H3K9 methyltransferase G9a associates with DNMT1 at the replication fork and acts to maintain H3K9me2 during replication (28). Thus, it is possible that maintenance of histone methylation patterns during MCE is also dependent on DNMT1. We analyzed the promoters of *Glut4* and *Fabp4* (aP2) by chromatin immunoprecipitation (ChIP) 2 days after induction of differentiation, and H3K9me2 levels near the transcription start sites were indeed reduced in DNMT1-silenced compared to control cells (Fig. 2B).

To assess whether DNMT1-dependent regulation of these chromatin marks has a functional role in the regulation of adipogenesis in 3T3-L1 cells, we compared gene expression in the presence or absence of DNMT1. In 3T3-L1 cells, DNMT1 mRNA levels were suppressed by 94% at day 0 (day of induction, 3 days after transfection) and by 88% at day 2 of differentiation, and protein levels of DNMT1 remained nearly undetectable at day 2 (Fig. 3C). Silencing of DNMT1 led to early induction of adipocyte-specific genes, such as those for Glut4, Fabp4, adiponectin, and adipsin, as well as early upregulation of the master regulator of adipogenesis PPARγ (Fig. 3A). Modestly higher levels of FASN and LDHA were also observed at day 2 of differentiation (Fig. 3A). Silencing of DNMT1 in C3H10T1/2 cells promoted increased expression of

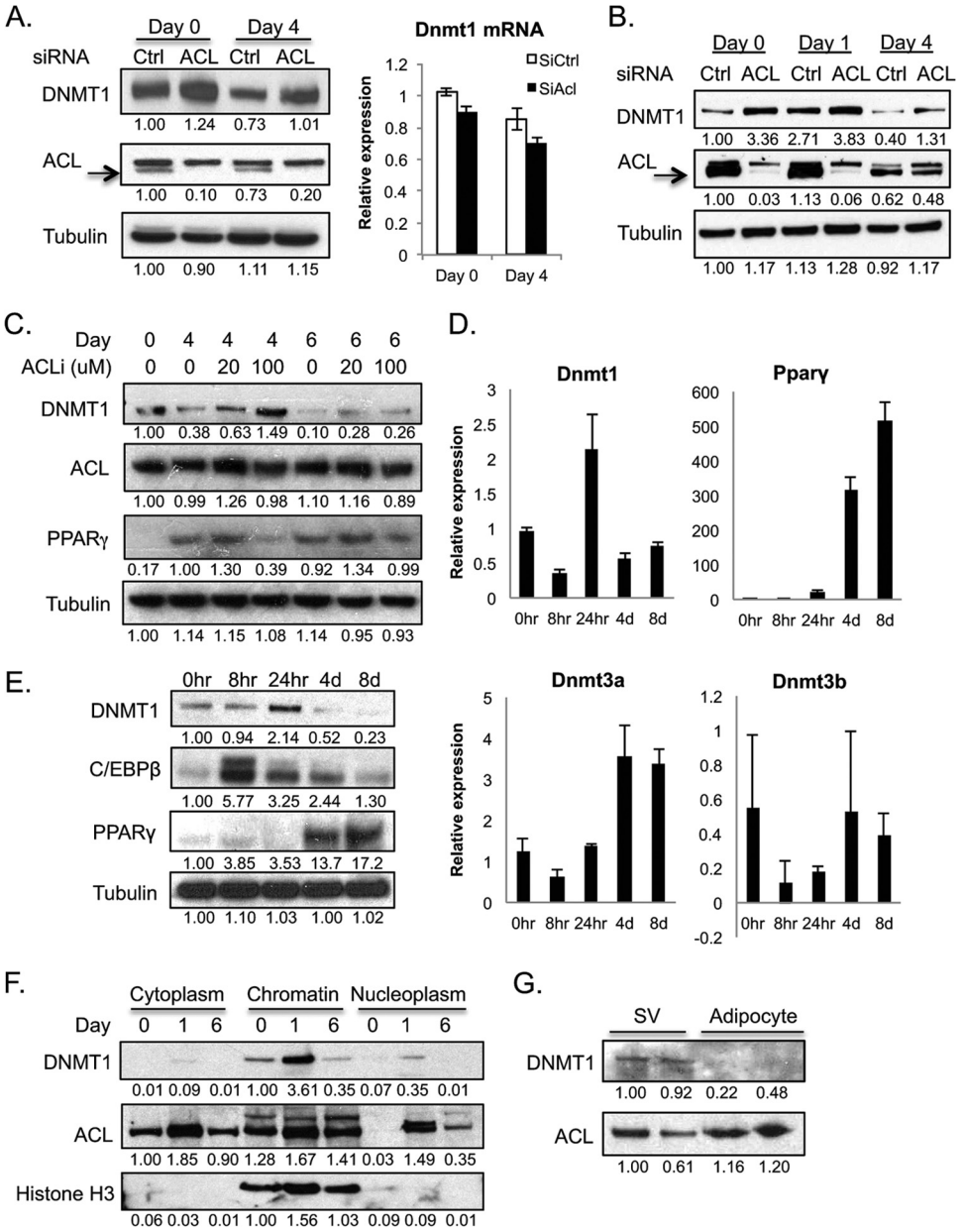

FIG 1 DNMT1 regulation during adipocyte differentiation. (A) 3T3-L1 preadipocytes were transfected with control and ACL-targeting siRNAs and stimulated to differentiate into adipocytes. DNMT1 protein and mRNA levels were assessed by Western blotting and quantitative reverse transcription-PCR (RT-PCR), respectively, at days 0 and 4 of differentiation. Q-PCR data were normalized to actin (mean ± standard deviation [SD] for triplicate samples). Data are representative of 3 independent repeats. (B) C3H10T1/2 cells were transfected with control and ACL-targeting siRNAs and adipocyte differentiation induced. DNMT1 levels were assessed by Western blotting. Similar results were obtained in 3 independent experiments. (C) 3T3-L1 cells were differentiated in the presence of the indicated doses of ACL inhibitor and analyzed by Western blotting. (D) RNA was isolated at the indicated time points after induction of differentiation in 3T3-L1 cells. Gene expression was analyzed by quantitative RT-PCR and normalized to actin (mean ± SD for triplicate samples). Data are representative of 2 independent experiments. (E) 3T3-L1 cells were lysed at different time points after induction of differentiation and analyzed by Western blotting. (F) Western blots showing cytoplasm, nucleoplasm, and chromatin fractions from differentiating 3T3-L1 cells. (G) Adipose tissue was harvested fresh from two mice and separated into stromal-vascular and adipocyte fractions. Lysates from each fraction were analyzed by Western blotting. The result is representative of 2 independent experiments.

adipocyte genes similar to that observed in 3T3-L1 cells (Fig. 3B). Some differences were observed in the sets of genes that are regulated by DNMT1 in 3T3-L1 cells and 10T1/2 cells, and effects of DNMT1 silencing in 10T1/2 cells were overall somewhat less pronounced than those in 3T3-L1 cells. These differences may reflect a differential need for DNMT1 activity in the two cell lines, since 10T1/2 cells do not undergo MCE and hence may not require DNMT1's maintenance methyltransferase activity but likely still utilize its scaffolding and repressor functions.

Phenotypically, lipid droplets were also visible earlier upon silencing of DNMT1, with small droplets apparent by 48 h after induction of differentiation (Fig. 3C). At this time point, few if any

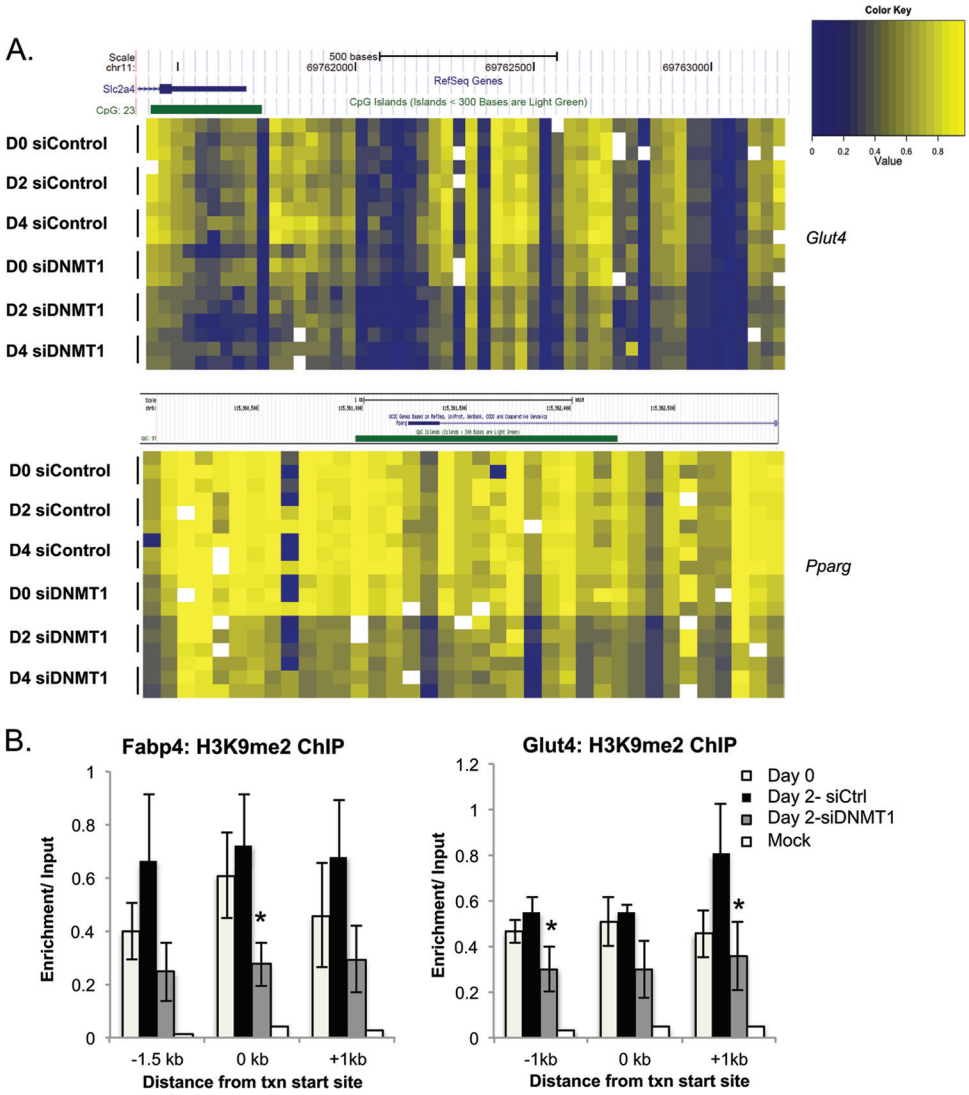

FIG 2 DNMT1 is critical for maintaining CpG methylation during early adipogenesis. 3T3-L1 preadipocytes were transfected with control and DNMT1 siRNAs and stimulated to differentiate into adipocytes. (A) Heat map representation of CpG methylation at the *Glut4* and *Pparg* loci at days 0, 2, and 4 after induction of differentiation in siCtrl- or siDNMT1-treated cells. Each row represents one of triplicate samples at each time point, and each column represents one of the 52 or 37 CpGs analyzed, for *Glut4* and *Pparg*, respectively. (B) H3K9me2 ChIP analysis of the *Fabp4* and *Glut4* genomic loci at day 2 of differentiation. Primers amplified DNA at the indicated distances from the transcriptional start sites. Data were normalized to input and represent triplicate samples (mean ± SD; *, $P < 0.05$). Data are representative of 2 independent repeats.

lipid droplets could be discerned in control cells (Fig. 3C). MCE still occurred in 3T3-L1 cells after silencing of DNMT1, though a small reduction in the final cell number was observed (Fig. 3D), consistent with DNMT1's role in proliferation (29). DNMT1 knockdown cells also consumed glucose at a rate comparable to or slightly higher than that of control cells upon induction of differentiation, indicating that DNMT1-silenced cells remain metabolically functional (Fig. 3E). Indeed, DNMT1-silenced adipocytes exhibited a similar capacity to take up glucose in response to insulin as control cells (Fig. 3F). These data suggest that DNMT1 functions during early adipogenesis to modulate the timing of induction of lineage-specific genes.

We next sought to determine the mechanism through which ACL regulates DNMT1 levels during differentiation. DNMT1 is an acetyl-protein, and acetylation of DNMT1 by the acetyltransferase Tip60 was shown to promote its association with the E3 ubiquitin ligase UHRF1, promoting DNMT1 ubiquitination and proteosomal degradation (15). Hence, higher levels of DNMT1 in the absence of ACL would be consistent with reduced acetylation (Fig. 1A). We first assessed whether Tip60 functionally regulates DNMT1 levels in 3T3-L1 cells. Indeed, similar to silencing of ACL (Fig. 1A), Tip60 silencing impaired suppression of DNMT1 protein levels during differentiation, without impacting DNMT1 mRNA levels (Fig. 4A). P/CAF has also been reported to be able to acetylate DNMT1 (16), although it has not been implicated in regulating DNMT1 stability. Consistently, DNMT1 levels could still be suppressed during differentiation after silencing of P/CAF (Fig. 4A). These data suggest the possibility that ACL regulates DNMT1 levels by modulating Tip60-dependent acetylation; however, it is also possible that ACL and Tip60 independently regulate

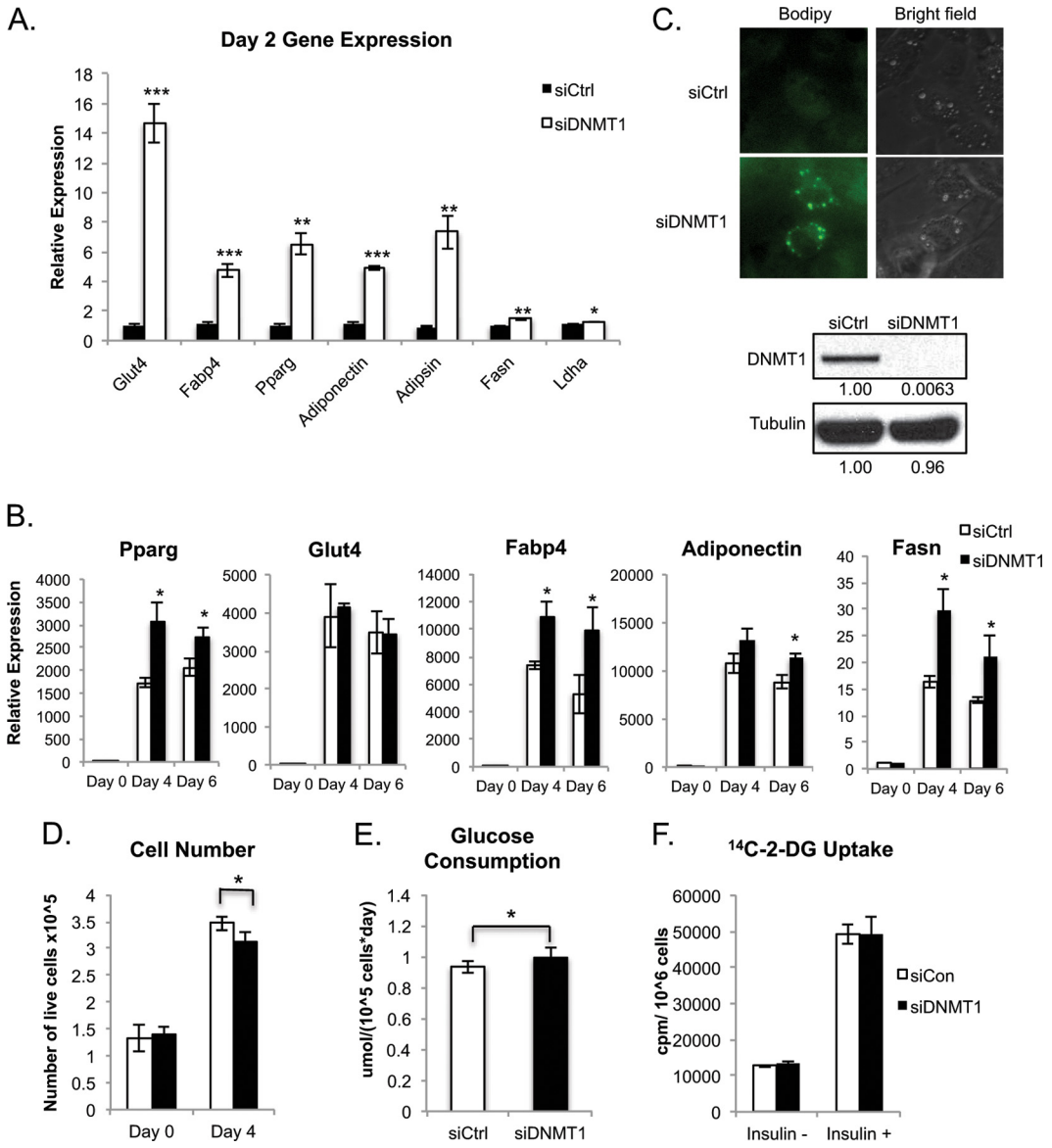

FIG 3 DNMT1 silencing accelerates adipogenesis. (A) 3T3-L1 preadipocytes were transfected with control or DNMT1-targeting siRNA and stimulated to differentiate into adipocytes. mRNA expression was analyzed by quantitative RT-PCR 2 days after induction of differentiation and normalized to 18S rRNA (mean ± SD for triplicate samples). Data are representative of 3 independent experiments. (B) Gene expression during adipocyte differentiation of C3H10T1/2 cells transfected with control and DNMT1-targeting siRNA and normalized to 18S rRNA (mean ± SD for triplicate samples). Similar results were obtained in 3 independent experiments. (C) Day 2 3T3-L1 cells were stained with Bodipy 493/503 and imaged. DNMT1 knockdown at day 2 is shown by Western blotting. (D) 3T3-L1 cells were counted at days 0 and 4 and graphed as means of triplicates ± SD. (E) Glucose consumption over the first 4 days of differentiation was also assessed. Data were normalized to cell number area under the curve from day 0 to 4, as described in Materials and Methods. Means of triplicate samples ± SD are graphed. Similar results were obtained in 2 independent experiments. (F) 2-Deoxy[^{14}C]glucose (^{14}C-2-DG) uptake was measured in siCtrl- and siDNMT1-transfected 3T3-L1 adipocytes at day 6 of differentiation. All statistical analyses are comparisons of 2 data sets and were performed using 2-tailed *t* tests (*, $P < 0.05$; **, $P < 0.005$; ***, $P < 0.0005$).

DNMT1 levels. We have previously observed that some, but not all, acetylation events are subject to control by acetyl-CoA availability (7). To test whether ACL regulates the acetylation levels of DNMT1, we silenced ACL in 293T cells and examined acetylation of myc-tagged DNMT1. Surprisingly, we failed to detect a difference in DNMT1 acetylation upon silencing of ACL or upon acetate supplementation, suggesting that DNMT1 acetylation may not be strongly regulated by acetyl-CoA availability (Fig. 4B). Since we did not observe ACL-dependent regulation of DNMT1 acetylation, we sought an alternative mechanism to explain the effects of ACL on DNMT1 protein levels.

DNMT1 has also been reported in the literature to be directly or indirectly targeted by microRNAs (30–36). One of these, miR-148a, has also been shown to be induced during adipocyte differentiation and has been identified as a potential PPARγ target (37, 38). miR-148a has been previously shown to directly repress DNMT1 by binding to its 3′ untranslated region (UTR) (30). While this was shown in human cells, the

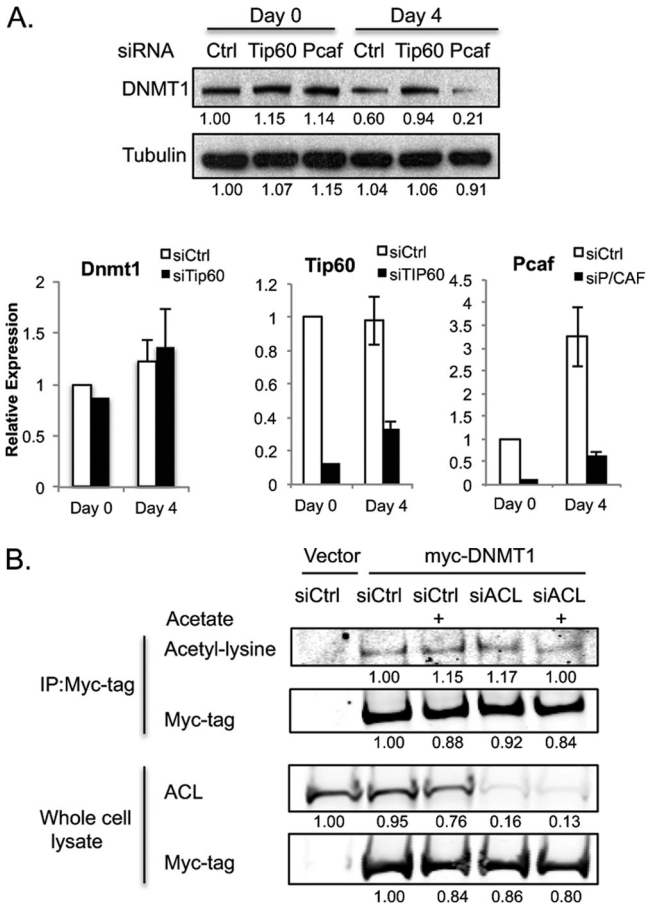

FIG 4 DNMT1 acetylation is not regulated upon silencing of ACL. (A) Total levels of DNMT1 were analyzed by Western blotting in 3T3-L1 cells at days 0 and 4 of differentiation, upon silencing of Tip60 or P/CAF. Q-PCR shows gene expression, with data normalized to 18S rRNA. Day 4 data represent the mean ± SD of triplicates. Similar results were obtained in 2 independent experiments. (B) HEK-293T cells were transfected with myc-DNMT1 or a control vector, as well as control or ACL targeting siRNA. Cells were treated for 24 h with 5 mM acetate. Acetylation of DNMT1 was assessed by immunoprecipitation of myc-DNMT1 and immunoblotting for acetyl lysine.

sequence targeted by miR-148a is conserved in the murine DNMT1 3′ UTR (Fig. 5A). Interestingly, a second site targeted by miR-148a was also identified in the protein-coding region of human DNMT1 (33), although this site is not conserved in mice. We found that miR-148a is induced during differentiation between days 2 and 4, correlating with downregulation of DNMT1 levels (Fig. 5B). In previous work, we showed that ACL modulates expression of certain genes, such as *Glut4*, during adipocyte differentiation (7). We therefore tested whether ACL might similarly regulate miR-148a expression during adipocyte differentiation, and we observed that, indeed, silencing of ACL blocked induction of the miR-148a primary transcript levels during differentiation (Fig. 5C). An ACL inhibitor also impaired induction of miR-148a expression (data not shown). The role of ACL in regulating miR-148a is not general among microRNAs, since another adipocyte differentiation-induced microRNA, miR-103-1 (38), was induced equally well in the presence or absence of ACL (Fig. 5C). Expression of miR-148a was partially rescued by treating cells with acetate, demonstrating that it is regulated in an acetyl-CoA-dependent manner (Fig. 5D).

The *Mir148a* gene is not located within an intron and thus may be regulated independently of other genes. We examined histone acetylation at the *Mir148a* gene in the presence or absence of ACL and found that levels of histone H4 acetylation are reduced upon silencing ACL and can be rescued with acetate treatment (Fig. 5E). To test whether miR-148a can regulate DNMT1 in adipocytes, we ectopically expressed miR-148a in preadipocytes and induced differentiation. Expression of miR-148a blocked the induction of DNMT1 during MCE, resulting in lower levels of DNMT1 protein at days 1 and 2 of differentiation (Fig. 5F).

We next investigated whether miR-148a overexpression is sufficient to mimic the effects of DNMT1 silencing on gene expression during differentiation. Indeed, similar to silencing of DNMT1, overexpression of miR-148a resulted in an early induction of gene expression in differentiating adipocytes, with clear effects observed at day 2 (Fig. 6A). Later in differentiation, adipocyte-specific gene expression was comparable for control and miR-148a-expressing genes (data not shown). Lipid accumulation was also markedly enhanced upon expression of miR-148a (Fig. 6B). Normally, adipocytes undergo growth arrest prior to the onset of lipid droplet formation; however, the early time point at which we observed lipid droplets forming seemed to overlap the MCE period. To determine whether lipid droplet-containing cells were able to undergo cell division upon expression of miR-148a, we treated cells with Bodipy lipid dye at 44 h after induction of differentiation and imaged them live for an additional 20 h. While many of the miR-148a-transfected cells containing lipid droplets were already growth arrested, lipid droplet-containing cells could be observed to undergo cell division (Fig. 6C). This was quantitated in an independent experiment by scoring approximately 1,000 cells within 6 fields for both miR-Ctrl- and miR-148a-transfected cells between 40 and 60 h after inducing differentiation. Cells were scored positive or negative for observed cell division and for visible lipid droplets. While the number of cells undergoing division during this time frame was not higher upon overexpression of miR-148a, lipid could be detected in more cells (~50% of cells versus ~20% of control cells) by 60 h after inducing differentiation (Fig. 6D). Cells with and without lipid droplets were equally likely to divide (Fig. 6D). Thus, lipid accumulation and cell division are not mutually exclusive in 3T3-L1 cells, and the results suggest a role for DNMT1 in segregating these processes in time by restraining adipocyte-specific gene expression during early adipogenesis.

Not surprisingly, miR-148a-mediated repression of DNMT1 was far less potent in reducing DNMT1 levels than siRNA-mediated silencing of DNMT1. Yet, similar effects on gene expression and lipid accumulation were observed with either DNMT1 silencing or miR-148a overexpression. MicroRNAs typically target multiple mRNAs in order to implement their effects, and it is likely that miR-148a has additional targets that promote differentiation. Accordingly, silencing of DNMT1 and expression of miR-148a produced additive effects on promoting early expression of adipocyte-specific genes (Fig. 7A). Nevertheless inhibition of miR-148a impaired the decrease in DNMT1 levels during differentiation, indicating that miR-148a is indeed important in regulating DNMT1 levels during normal differentiation (Fig. 7B). miR-148a-dependent suppression of DNMT1 does not appear to be

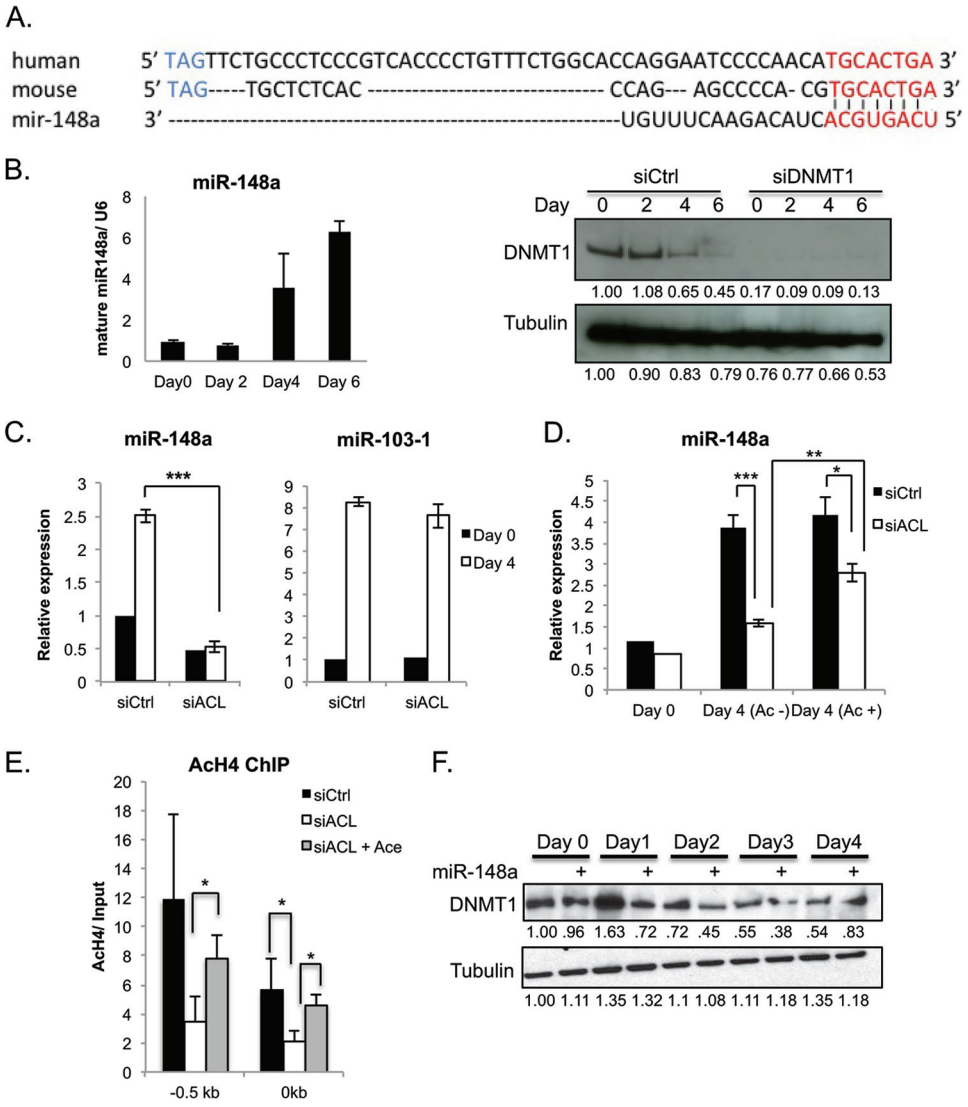

FIG 5 miR-148a targets DNMT1 and is regulated by ACL. (A) The miR-148a target sequence is conserved in the mouse and human DNMT1 3′ UTRs. The miR-148a target sequence is shown in red, and the stop codon is in blue. (B) RNA was isolated from 3T3-L1 cells at the indicated time points after induction of differentiation and levels of mature miR-148a assessed from triplicate samples, normalized to U6 (mean ± SD). In parallel, 3T3-L1 preadipocytes were transfected with control and DNMT1 siRNAs, and differentiated. DNMT1 levels were analyzed by Western blotting. (C) 3T3-L1 preadipocytes were transfected with control and ACL siRNAs and stimulated to differentiate into adipocytes. RNA was harvested at days 0 and 4 days and primary transcript levels of miR-148a and miR-103-1 assessed from triplicate wells, normalized to 18S rRNA (mean ± SD). (D) 3T3-L1 cells were transfected with control and ACL siRNAs and differentiated in the presence or absence of 5 mM sodium acetate. Primary transcript levels of miR-148a were assessed in triplicate, normalized to 18S rRNA (mean ± SD). (E) Control and ACL siRNAs were transfected into 3T3-L1 cells and cells differentiated for 4 days with or without 5 mM acetate. AcH4 ChIP was performed to analyze the miR-148a locus at the transcriptional start site (0 kb) and 500 bp upstream, and data were normalized to input. Data represent triplicate samples (mean ± SD). (F) miR-148a and miR-Ctrl were transfected into 3T3-L1 preadipocytes and cells differentiated. DNMT1 protein levels were analyzed by Western blotting at the indicated time points. These data are representative of 2 independent experimental repeats. All statistical analyses represent comparisons of 2 data sets and were performed using 2-tailed *t* tests (*, $P < 0.05$; **, $P < 0.005$;***, $P < 0.0005$).

required for differentiation, however, since expression of differentiation markers was not different in control LNA and miR-148a LNA inhibitor-transfected cells, consistent with the model that miR-148a serves to suppress DNMT1 after it is no longer functionally required (Fig. 7B). Similarly, modest overexpression of DNMT1, accomplished by retroviral transduction of preadipocytes, did not suppress the cells' capacity to differentiate, indicating that the normal amounts of DNMT1 are sufficient to accomplish DNMT1's functions, and the presence of somewhat more DNMT1 does not impair differentiation (Fig. 7C). Overexpression of DNMT1 at high levels or stable overexpression of DNMT1 was not consistent with preadipocyte viability, and hence differentiation could not be tested under these conditions.

Although modest DNMT1 overexpression did not suppress differentiation, inhibition of histone demethylation causes histone hypermethylation, which does impair adipogenesis (8). Isocitrate dehydrogenase (*IDH1* and *IDH2*) mutations occur in certain types of cancer and cause hypermethylation of histones and DNA. These epigenetic changes occur because the mutant IDH enzymes produce high levels of the metabolite 2-hydroxy-

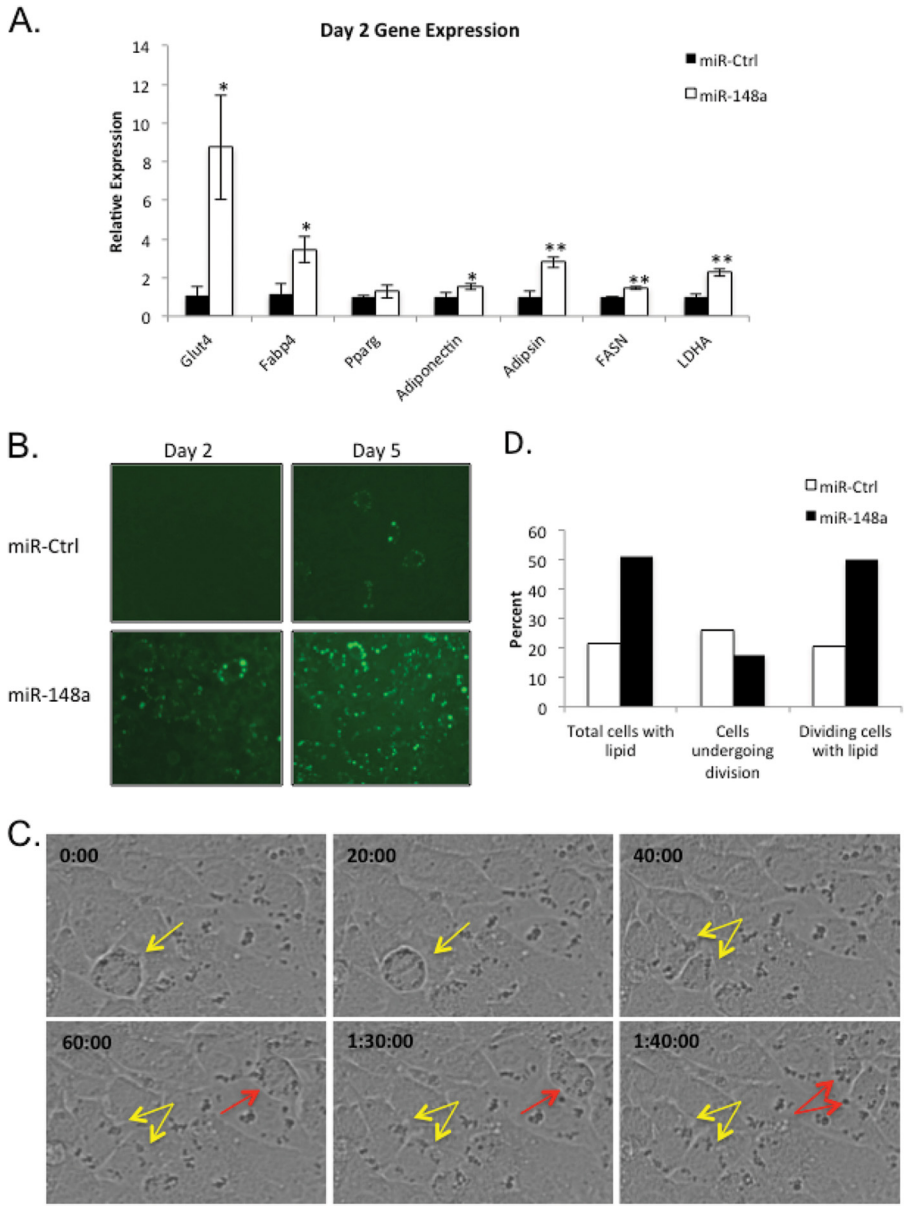

FIG 6 Ectopic expression of miR-148a accelerates adipocyte differentiation. miR-148a and miR-Ctrl were transfected into 3T3-L1 preadipocytes and cells differentiated. (A) Day 2 gene expression was assessed by Q-PCR and normalized to 18S rRNA (mean ± SD for triplicate samples). Statistical analyses are comparisons of 2 data sets and were performed using *t* tests (*, $P < 0.05$; **, $P < 0.005$). Similar results were obtained in at least 3 independent experiments. (B) Bodipy lipid staining in live cells at 2 and 5 days after induction of differentiation. (C) Cells ectopically expressing miR-148a were imaged live beginning 44 h after induction of differentiation. Frames from the first 100 min of filming are shown, with arrows indicating 2 lipid droplet-containing cells dividing. (D) Cells (~1,000/condition) were scored for lipid and cell division from hours 40 to 60 of differentiation. Results are presented as percentage of total.

glutarate (2-HG), which inhibits Jmjc histone demethylases and TET proteins, which are implicated in DNA demethylation (8, 39–41). Expression of mutant IDH proteins in 3T3-L1 adipocytes results in a hypermethylation phenotype and differentiation block (8). We therefore reasoned that if miR-148a can promote differentiation through regulation of DNA and histone methylation, it might be able to reverse the hypermethylation-mediated differentiation block caused by mutant IDH (Fig. 8A). Strikingly, in 3T3-L1 cells with IDH2-R140Q or IDH2-R172K mutants, overexpression of miR-148a partially restored differentiation, as assessed by lipid accumulation and gene expression (Fig. 8B and C). Additionally, histone methylation levels were normalized upon miR-148a expression (Fig. 8D). Hence, miR-148a can partially rescue an epigenetically mediated differentiation block.

DISCUSSION

In previous work we have shown a key role for ACL in the regulation of histone acetylation levels during adipocyte differentiation (7). In this study, we show that ACL activity also

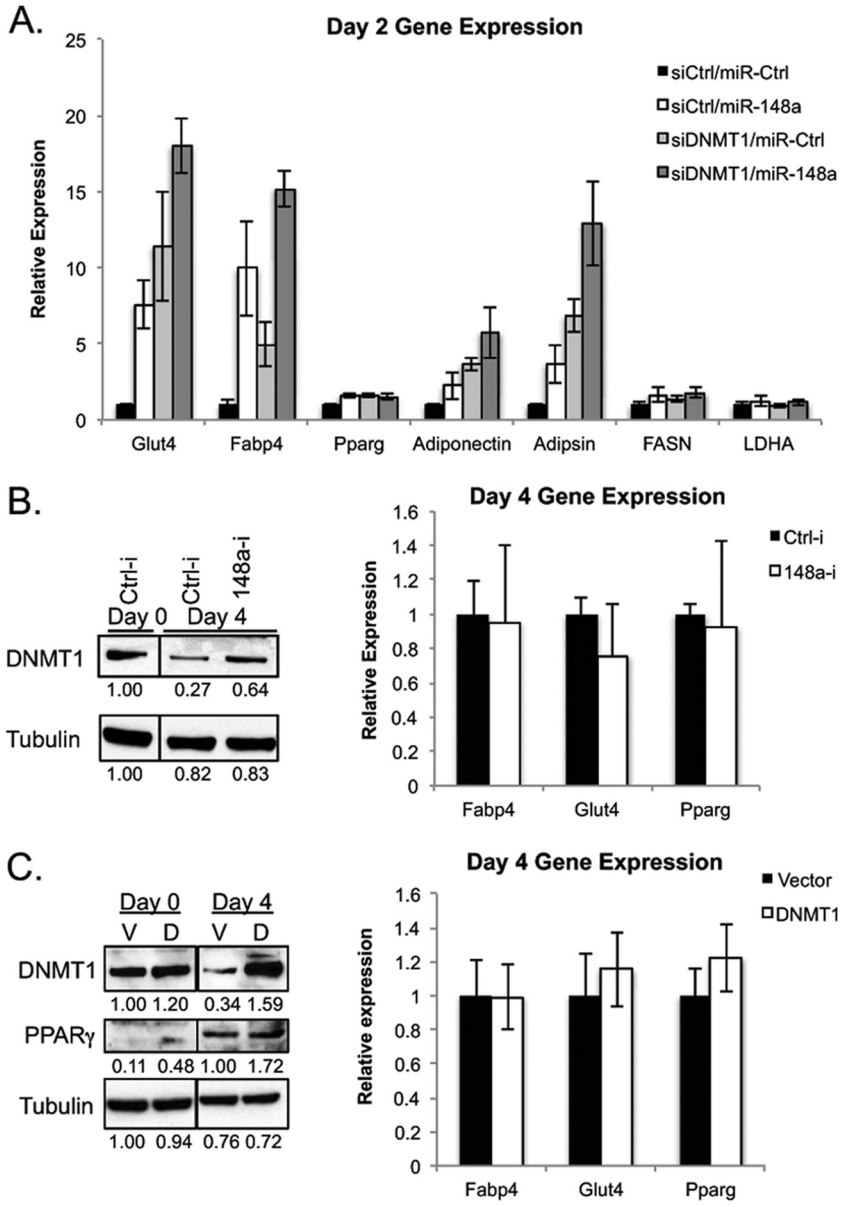

FIG 7 Additive effects of miR-148a expression and DNMT1 silencing on adipocyte differentiation. (A) Gene expression at day 2 of differentiation in 3T3-L1 cells transfected with combinations of siCtrl/siDNMT1 plus miR-Ctrl/miR-148a. Data were normalized to 18S rRNA (mean ± SD of triplicates). (B) 3T3-L1 cells were transfected with miR-Ctrl and miR-148a-targeting LNA inhibitors and differentiated. DNMT1 levels were assessed by Western blotting. Gene expression was assessed at day 4 of differentiation, normalized to 18S rRNA (mean ± SD of triplicates). (C) 3T3-L1 cells were transduced with retrovirus expressing DNMT1 (D) or empty vector (V). At 3 days after infection, cells were differentiated for 4 days. DNMT1 levels were analyzed by Western blotting. Gene expression was measured by Q-PCR and normalized to 18S (mean ± SD of triplicates).

modulates levels of DNMT1 during adipocyte differentiation. Investigation of the role of DNMT1 during adipocyte differentiation demonstrated that DNMT1 expression is important for maintaining DNA and H3K9 methylation during the mitotic clonal expansion phase of adipocyte differentiation. Maintaining DNA methylation during MCE restrains inappropriate activation of adipocyte-specific gene expression and lipid accumulation while cells are dividing, and DNMT1 silencing results in accelerated adipocyte differentiation.

It is not fully clear why it would be advantageous to inhibit induction of adipocyte-specific genes early in differentiation. High glucose consumption in adipocytes has been shown to result in elevated production of reactive oxygen species (ROS) (42). It is possible that by preventing cells from taking on their metabolic functions during the mitotic clonal expansion period, ROS-induced damage to DNA during MCE might be minimized. Perhaps more likely is that methylation may serve to ensure that adipocyte-specific genes are repressed until cells receive appropriate signals to differentiate. This interpretation is consistent with a study by Taylor and Jones (21), which showed spontaneous adipocyte differentiation after treatment with DNMT inhibitors. We observed that about 50% of CpGs within the *Glut4* promoter and 80% of

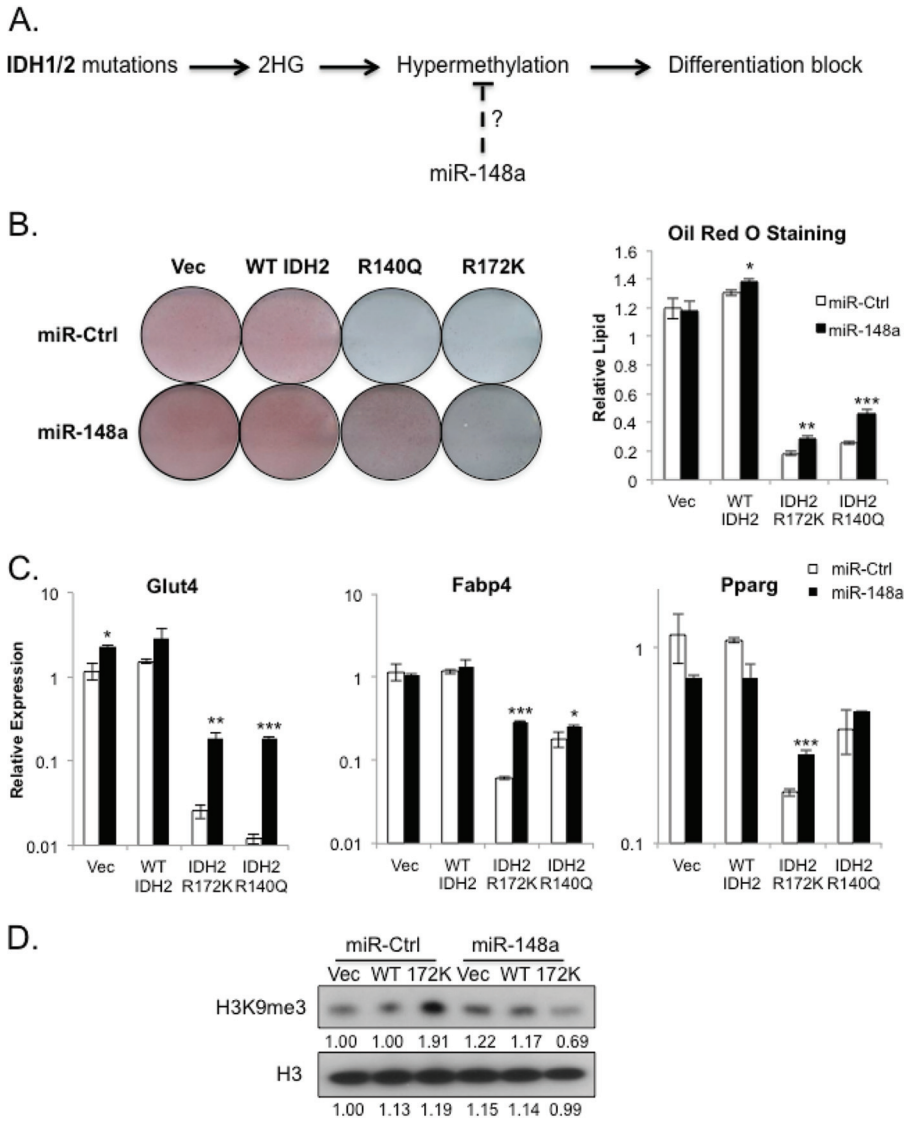

FIG 8 miR-148a overcomes a hypermethylation-mediated differentiation block. (A) 2-HG produced by mutant IDH enzymes inhibits Jmjc histone demethylases and TET proteins, resulting in a hypermethylation phenotype in cells expressing mutant IDH. These changes result in a differentiation block in cancer cells, as well as in adipocytes. We hypothesized that miR-148a might reverse the hypermethylation phenotype and restore the ability of IDH mutant-expressing 3T3-L1 cells to differentiate. (B) Stable 3T3-L1 cell lines expressing wild-type (WT) or mutant forms of IDH were transfected with miR-Ctrl or miR-148a. Cells were differentiated for 6 days, fixed, and stained with Oil Red O. Oil Red O staining was quantified from triplicate experiments. (C) Gene expression was quantified under the same conditions (mean from triplicate wells ± SD). (D) H3K9me3 levels were analyzed by Western blotting in day 0 preadipocytes. All statistical analyses represent comparisons of 2 data sets and were performed using 2-tailed *t* tests (*, $P < 0.05$; **, $P < 0.005$; ***, $P < 0.0005$).

those at *Pparg* were methylated (Fig. 2A), and relatively high (at least 50%) methylation was previously observed at the adiponectin and CEBPα promoters in adipocytes as well (8). Hence, maintaining relatively high levels of methylation at promoters of adipocyte-specific genes could serve as a mechanism to suppress induction of these genes until certain signaling conditions are met. For example, *in vivo*, precursor cells contained in the stromal-vascular compartment of adipose tissue express the adipogenic transcription factor PPARγ (43), which is necessary and sufficient for adipogenesis (1), yet these progenitor cells presumably remain undifferentiated until receipt of cues to differentiate. Consistent with the possibility that DNA methylation restrains inappropriate differentiation, gene ontology analysis of highly methylated genes showed enrichment for genes involved in physiological responses to stimuli (44). Hence, we speculate that DNMT1-dependent DNA methylation may serve to silence these adipocyte-specific genes, even if PPARγ is expressed, until cells receive the proper signaling cues to differentiate.

Mitotic clonal expansion is critical for differentiation of 3T3-L1 cells and MEFs into adipocytes (1, 3). In humans, new adipocyte formation occurs throughout childhood and adolescence, with fat cell numbers plateauing around age 20, regardless of body fat mass (45). Adipocytes are replaced in adults at a rate of about 10% each year, indicating that some new differentiation occurs throughout the life span (45). Whether MCE is also important for adipogenesis *in vivo* is not fully clear, although some evi-

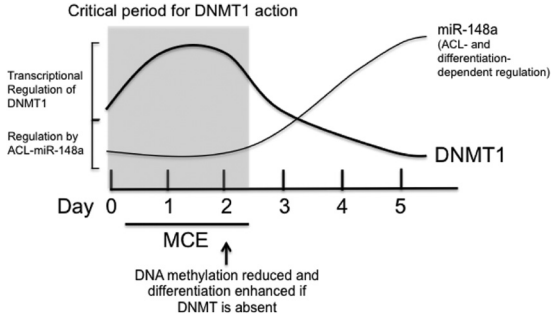

FIG 9 Model. DNMT1 maintains methylation patterns during early adipocyte differentiation and is suppressed later in differentiation by ACL-dependent regulation of miR-148a. DNMT1 plays a role in maintaining methylation patterns and restraining adipocyte-specific gene expression and lipid accumulation during early adipogenesis. If DNMT1 is absent, differentiation is accelerated. Later in differentiation, DNMT1 may no longer be necessary, and its levels are suppressed. Suppression of DNMT1 occurs through both transcriptional and posttranscriptional mechanisms. ACL mediates posttranscriptional suppression of DNMT1 levels by promoting expression of miR-148a.

dence suggests that it may play a role. For example, mice lacking E2F1, a transcription factor important for MCE, exhibit reduced body weight and fat weight gain when fed a high-fat diet (46). Regardless, PPARγ-expressing preadipocytes do divide *in vivo* (43), and DNMT1 is expected to be important in these cells for sustaining DNA methylation patterns. Consistently, DNMT1 levels are higher in the preadipocyte-containing stromal-vascular fraction of adipose tissue than in adipocytes (Fig. 1G).

The results of this study indicate that ACL regulates DNMT1 protein levels in addition to histone acetylation levels during adipocyte differentiation (Fig. 9). In professional metabolic cells such as adipocytes, regulating chromatin modifications in a nutrient-responsive manner may allow environmental modulation of gene expression. In support of this possibility, we have previously shown that ACL modulates the expression of a subset of genes involved in glucose metabolism, allowing nutrient-sensitive acetyl-CoA production to influence metabolic gene expression (7). The extent to which ACL-dependent regulation of DNMT1 regulates histone and DNA methylation levels is not yet clear, since ACL seems to function in downregulating DNMT1 levels later in differentiation when it is no longer required for the maintenance of methylation patterns during DNA replication. Inhibition of miR-148a does not suppress differentiation, suggesting that DNMT1's primary role is in the early part of differentiation. On the other hand, expression of mutant IDH proteins in preadipocytes results in hypermethylation and inhibition of capacity to differentiate. miR-148a partially rescues differentiation and restores normal histone methylation levels in these cells, likely through regulation of DNMT1 and additional targets. Interestingly, silencing of DNMT1 was not sufficient to restore differentiation in this context, highlighting the notion that microRNAs mediate their effects through regulation of networks of genes. More work is needed to understand the mechanisms through which this occurs, as well as whether miR-148a or other microRNAs could provide any therapeutic benefit in the context of IDH mutant cancers. Notably, miR-148a has been reported to promote both myogenesis and osteoclastogenesis (47, 48), suggesting that it can promote differentiation in multiple contexts. miR-148a is also suppressed in several types of cancer (49–55). Reexpression of miR-148a in cancer cells may promote a more differentiated state, since the epithelial-to-mesenchymal transition was suppressed upon expression of miR-148a in both hepatocellular carcinoma and non-small-cell lung cancer cells (55, 56).

In summary, this study demonstrates that DNMT1 is critical for maintaining DNA and histone H3K9 methylation levels during MCE and that it plays a role in restraining adipocyte-specific gene expression and lipid accumulation during early adipogenesis. Hence, DNMT1 may be a key player in separating proliferation and lipid accumulation temporally during 3T3-L1 differentiation. We also show that ACL contributes to the downregulation of DNMT1 protein levels after MCE and that this occurs at least in part through regulation of miR-148a, which targets DNMT1. miR-148a also promotes differentiation, likely through regulation of DNMT1 and other targets.

ACKNOWLEDGMENTS

K.E.W. is supported by the Penn Diabetes Research Center (pilot grant allocated from P30 DK19525), the American Diabetes Association (7-12-JF-59), the Pew Charitable Trusts, and University of Pennsylvania Start-Up funds. C.B.T. received grant support from the MSKCC General Fund.

C.B.T. is a founder and consultant of Agios Pharmaceuticals and has a financial interest in Agios.

The content of this paper is solely the responsibility of the authors and does not necessarily represent the official views of the National Institutes of Health.

We thank Mitch Lazar for critical reading of the manuscript and members of the Wellen and Thompson labs for helpful discussions. We are grateful to the Epigenomics Core Facility of Weill Cornell Medical College for performing the bisulfite sequencing and to M. E. Figueroa for help with the heat map data presentation. Z. Wang generously provided the myc-DNMT1 construct. We are also grateful to C. Sterner and L. Chodosh for kindly donating spare mice from their colony for the experiment for Fig. 1G.

REFERENCES

1. **Lefterova MI, Lazar MA.** 2009. New developments in adipogenesis. Trends Endocrinol. Metab. **20:**107–114.
2. **Rosen ED, MacDougald OA.** 2006. Adipocyte differentiation from the inside out. Nat. Rev. Mol. Cell Biol. **7:**885–896.
3. **Tang QQ, Lane MD.** 2012. Adipogenesis: from stem cell to adipocyte. Annu. Rev. Biochem. **81:**715–736.
4. **Mikkelsen TS, Xu Z, Zhang X, Wang L, Gimble JM, Lander ES, Rosen ED.** 2010. Comparative epigenomic analysis of murine and human adipogenesis. Cell **143:**156–169.
5. **Steger DJ, Grant GR, Schupp M, Tomaru T, Lefterova MI, Schug J, Manduchi E, Stoeckert CJ, Jr, Lazar MA.** 2010. Propagation of adipogenic signals through an epigenomic transition state. Genes Dev. **24:**1035–1044.
6. **Siersbaek R, Nielsen R, Mandrup S.** 2012. Transcriptional networks and chromatin remodeling controlling adipogenesis. Trends Endocrinol. Metab. **23:**56–64.
7. **Wellen KE, Hatzivassiliou G, Sachdeva UM, Bui TV, Cross JR, Thompson CB.** 2009. ATP-citrate lyase links cellular metabolism to histone acetylation. Science **324:**1076–1080.
8. **Lu C, Ward PS, Kapoor GS, Rohle D, Turcan S, Abdel-Wahab O, Edwards CR, Khanin R, Figueroa ME, Melnick A, Wellen KE, O'Rourke DM, Berger SL, Chan TA, Levine RL, Mellinghoff IK, Thompson CB.** 2012. IDH mutation impairs histone demethylation and results in a block to cell differentiation. Nature **483:**474–478.
9. **Choudhary C, Kumar C, Gnad F, Nielsen ML, Rehman M, Walther TC, Olsen JV, Mann M.** 2009. Lysine acetylation targets protein complexes and co-regulates major cellular functions. Science **325:**834–840.

10. **Kim SC, Sprung R, Chen Y, Xu Y, Ball H, Pei J, Cheng T, Kho Y, Xiao H, Xiao L, Grishin NV, White M, Yang XJ, Zhao Y.** 2006. Substrate and functional diversity of lysine acetylation revealed by a proteomics survey. Mol. Cell **23:**607–618.
11. **Yang L, Vaitheesvaran B, Hartil K, Robinson AJ, Hoopmann MR, Eng JK, Kurland IJ, Bruce JE.** 2011. The fasted/fed mouse metabolic acetylome: N6-acetylation differences suggest acetylation coordinates organ-specific fuel switching. J. Proteome Res. **10:**4134–4149.
12. **Zhao S, Xu W, Jiang W, Yu W, Lin Y, Zhang T, Yao J, Zhou L, Zeng Y, Li H, Li Y, Shi J, An W, Hancock SM, He F, Qin L, Chin J, Yang P, Chen X, Lei Q, Xiong Y, Guan KL.** 2010. Regulation of cellular metabolism by protein lysine acetylation. Science **327:**1000–1004.
13. **Guan KL, Xiong Y.** 2011. Regulation of intermediary metabolism by protein acetylation. Trends Biochem. Sci. **36:**108–116.
14. **Jiang W, Wang S, Xiao M, Lin Y, Zhou L, Lei Q, Xiong Y, Guan KL, Zhao S.** 2011. Acetylation regulates gluconeogenesis by promoting PEPCK1 degradation via recruiting the UBR5 ubiquitin ligase. Mol. Cell **43:**33–44.
15. **Du Z, Song J, Wang Y, Zhao Y, Guda K, Yang S, Kao HY, Xu Y, Willis J, Markowitz SD, Sedwick D, Ewing RM, Wang Z.** 2010. DNMT1 stability is regulated by proteins coordinating deubiquitination and acetylation-driven ubiquitination. Sci. Signal. **3:**ra80. doi:10.1126/scisignal.2001462.
16. **Peng L, Yuan Z, Ling H, Fukasawa K, Robertson K, Olashaw N, Koomen J, Chen J, Lane WS, Seto E.** 2011. SIRT1 deacetylates the DNA methyltransferase 1 (DNMT1) protein and alters its activities. Mol. Cell. Biol. **31:**4720–4734.
17. **Li E, Bestor TH, Jaenisch R.** 1992. Targeted mutation of the DNA methyltransferase gene results in embryonic lethality. Cell **69:**915–926.
18. **Okano M, Bell DW, Haber DA, Li E.** 1999. DNA methyltransferases Dnmt3a and Dnmt3b are essential for de novo methylation and mammalian development. Cell **99:**247–257.
19. **Baylin SB, Jones PA.** 2011. A decade of exploring the cancer epigenome—biological and translational implications. Nat. Rev. Cancer **11:**726–734.
20. **Rodriguez-Paredes M, Esteller M.** 2011. Cancer epigenetics reaches mainstream oncology. Nat. Med. **17:**330–339.
21. **Taylor SM, Jones PA.** 1979. Multiple new phenotypes induced in 10T1/2 and 3T3 cells treated with 5-azacytidine. Cell **17:**771–779.
22. **Guo W, Zhang KM, Tu K, Li YX, Zhu L, Xiao HS, Yang Y, Wu JR.** 2009. Adipogenesis licensing and execution are disparately linked to cell proliferation. Cell Res. **19:**216–223.
23. **Jain M, Nilsson R, Sharma S, Madhusudhan N, Kitami T, Souza AL, Kafri R, Kirschner MW, Clish CB, Mootha VK.** 2012. Metabolite profiling identifies a key role for glycine in rapid cancer cell proliferation. Science **336:**1040–1044.
24. **Hatzivassiliou G, Zhao F, Bauer DE, Andreadis C, Shaw AN, Dhanak D, Hingorani SR, Tuveson DA, Thompson CB.** 2005. ATP citrate lyase inhibition can suppress tumor cell growth. Cancer Cell **8:**311–321.
25. **Wellen KE, Fucho R, Gregor MF, Furuhashi M, Morgan C, Lindstad T, Vaillancourt E, Gorgun CZ, Saatcioglu F, Hotamisligil GS.** 2007. Coordinated regulation of nutrient and inflammatory responses by STAMP2 is essential for metabolic homeostasis. Cell **129:**537–548.
26. **Wysocka J, Reilly PT, Herr W.** 2001. Loss of HCF-1-chromatin association precedes temperature-induced growth arrest of tsBN67 cells. Mol. Cell. Biol. **21:**3820–3829.
27. **Shaknovich R, Cerchietti L, Tsikitas L, Kormaksson M, De S, Figueroa ME, Ballon G, Yang SN, Weinhold N, Reimers M, Clozel T, Luttrop K, Ekstrom TJ, Frank J, Vasanthakumar A, Godley LA, Michor F, Elemento O, Melnick A.** 2011. DNA methyltransferase 1 and DNA methylation patterning contribute to germinal center B-cell differentiation. Blood **118:**3559–3569.
28. **Esteve PO, Chin HG, Smallwood A, Feehery GR, Gangisetty O, Karpf AR, Carey MF, Pradhan S.** 2006. Direct interaction between DNMT1 and G9a coordinates DNA and histone methylation during replication. Genes Dev. **20:**3089–3103.
29. **Chen T, Hevi S, Gay F, Tsujimoto N, He T, Zhang B, Ueda Y, Li E.** 2007. Complete inactivation of DNMT1 leads to mitotic catastrophe in human cancer cells. Nat. Genet. **39:**391–396.
30. **Braconi C, Huang N, Patel T.** 2010. MicroRNA-dependent regulation of DNA methyltransferase-1 and tumor suppressor gene expression by interleukin-6 in human malignant cholangiocytes. Hepatology **51:**881–890.
31. **Garzon R, Liu S, Fabbri M, Liu Z, Heaphy CE, Callegari E, Schwind S, Pang J, Yu J, Muthusamy N, Havelange V, Volinia S, Blum W, Rush LJ, Perrotti D, Andreeff M, Bloomfield CD, Byrd JC, Chan K, Wu LC, Croce CM, Marcucci G.** 2009. MicroRNA-29b induces global DNA hypomethylation and tumor suppressor gene reexpression in acute myeloid leukemia by targeting directly DNMT3A and 3B and indirectly DNMT1. Blood **113:**6411–6418.
32. **Huang J, Wang Y, Guo Y, Sun S.** 2010. Down-regulated microRNA-152 induces aberrant DNA methylation in hepatitis B virus-related hepatocellular carcinoma by targeting DNA methyltransferase 1. Hepatology **52:**60–70.
33. **Pan W, Zhu S, Yuan M, Cui H, Wang L, Luo X, Li J, Zhou H, Tang Y, Shen N.** 2010. MicroRNA-21 and microRNA-148a contribute to DNA hypomethylation in lupus CD4+ T cells by directly and indirectly targeting DNA methyltransferase 1. J. Immunol. **184:**6773–6781.
34. **Wang H, Wu J, Meng X, Ying X, Zuo Y, Liu R, Pan Z, Kang T, Huang W.** 2011. MicroRNA-342 inhibits colorectal cancer cell proliferation and invasion by directly targeting DNA methyltransferase 1. Carcinogenesis **32:**1033–1042.
35. **Wang YS, Chou WW, Chen KC, Cheng HY, Lin RT, Juo SH.** 2012. MicroRNA-152 mediates DNMT1-regulated DNA methylation in the estrogen receptor alpha gene. PLoS One **7:**e30635. doi:10.1371/journal.pone.0030635.
36. **Zhao S, Wang Y, Liang Y, Zhao M, Long H, Ding S, Yin H, Lu Q.** 2011. MicroRNA-126 regulates DNA methylation in CD4+ T cells and contributes to systemic lupus erythematosus by targeting DNA methyltransferase 1. Arthritis Rheum. **63:**1376–1386.
37. **John E, Wienecke-Baldacchino A, Liivrand M, Heinaniemi M, Carlberg C, Sinkkonen L.** 2012. Dataset integration identifies transcriptional regulation of microRNA genes by PPARgamma in differentiating mouse 3T3-L1 adipocytes. Nucleic Acids Res. **40:**4446–4460.
38. **Xie H, Lim B, Lodish HF.** 2009. MicroRNAs induced during adipogenesis that accelerate fat cell development are downregulated in obesity. Diabetes **58:**1050–1057.
39. **Dang L, White DW, Gross S, Bennett BD, Bittinger MA, Driggers EM, Fantin VR, Jang HG, Jin S, Keenan MC, Marks KM, Prins RM, Ward PS, Yen KE, Liau LM, Rabinowitz JD, Cantley LC, Thompson CB, Vander Heiden MG, Su SM.** 2009. Cancer-associated IDH1 mutations produce 2-hydroxyglutarate. Nature **462:**739–744.
40. **Figueroa ME, Abdel-Wahab O, Lu C, Ward PS, Patel J, Shih A, Li Y, Bhagwat N, Vasanthakumar A, Fernandez HF, Tallman MS, Sun Z, Wolniak K, Peeters JK, Liu W, Choe SE, Fantin VR, Paietta E, Lowenberg B, Licht JD, Godley LA, Delwel R, Valk PJ, Thompson CB, Levine RL, Melnick A.** 2010. Leukemic IDH1 and IDH2 mutations result in a hypermethylation phenotype, disrupt TET2 function, and impair hematopoietic differentiation. Cancer Cell **18:**553–567.
41. **Ward PS, Patel J, Wise DR, Abdel-Wahab O, Bennett BD, Coller HA, Cross JR, Fantin VR, Hedvat CV, Perl AE, Rabinowitz JD, Carroll M, Su SM, Sharp KA, Levine RL, Thompson CB.** 2010. The common feature of leukemia-associated IDH1 and IDH2 mutations is a neomorphic enzyme activity converting alpha-ketoglutarate to 2-hydroxyglutarate. Cancer Cell **17:**225–234.
42. **Lin Y, Berg AH, Iyengar P, Lam TK, Giacca A, Combs TP, Rajala MW, Du X, Rollman B, Li W, Hawkins M, Barzilai N, Rhodes CJ, Fantus IG, Brownlee M, Scherer PE.** 2005. The hyperglycemia-induced inflammatory response in adipocytes: the role of reactive oxygen species. J. Biol. Chem. **280:**4617–4626.
43. **Tang W, Zeve D, Suh JM, Bosnakovski D, Kyba M, Hammer RE, Tallquist MD, Graff JM.** 2008. White fat progenitor cells reside in the adipose vasculature. Science **322:**583–586.
44. **Zhang Y, Rohde C, Tierling S, Jurkowski TP, Bock C, Santacruz D, Ragozin S, Reinhardt R, Groth M, Walter J, Jeltsch A.** 2009. DNA methylation analysis of chromosome 21 gene promoters at single base pair and single allele resolution. PLoS Genet. **5:**e1000438. doi:10.1371/journal.pgen.1000438.
45. **Spalding KL, Arner E, Westermark PO, Bernard S, Buchholz BA, Bergmann O, Blomqvist L, Hoffstedt J, Naslund E, Britton T, Concha H, Hassan M, Ryden M, Frisen J, Arner P.** 2008. Dynamics of fat cell turnover in humans. Nature **453:**783–787.
46. **Fajas L, Landsberg RL, Huss-Garcia Y, Sardet C, Lees JA, Auwerx J.** 2002. E2Fs regulate adipocyte differentiation. Dev. Cell **3:**39–49.
47. **Cheng P, Chen C, He HB, Hu R, Zhou HD, Xie H, Zhu W, Dai RC, Wu XP, Liao EY, Luo XH.** 2013. miR-148a regulates osteoclastogenesis by

targeting V-maf musculoaponeurotic fibrosarcoma oncogene homolog B. J. Bone Miner. Res. **28:**1180–1190.
48. **Zhang J, Ying ZZ, Tang ZL, Long LQ, Li K.** 2012. MicroRNA-148a promotes myogenic differentiation by targeting the ROCK1 gene. J. Biol. Chem. **287:**21093–21101.
49. **Aydogdu E, Katchy A, Tsouko E, Lin CY, Haldosen LA, Helguero L, Williams C.** 2012. MicroRNA-regulated gene networks during mammary cell differentiation are associated with breast cancer. Carcinogenesis **33:** 1502–1511.
50. **LaConti JJ, Shivapurkar N, Preet A, Deslattes Mays A, Peran I, Kim SE, Marshall JL, Riegel AT, Wellstein A.** 2011. Tissue and serum microRNAs in the Kras(G12D) transgenic animal model and in patients with pancreatic cancer. PLoS One **6:**e20687. doi:10.1371/journal.pone.0020687.
51. **Liffers, ST, JB. Munding, M. Vogt, JD. Kuhlmann, B. Verdoodt, S. Nambiar, A. Maghnouj, A. Mirmohammadsadegh, SA. Hahn, and A. Tannapfel.** 2011. MicroRNA-148a is down-regulated in human pancreatic ductal adenocarcinomas and regulates cell survival by targeting CDC25B. Lab. Invest. **91:**1472–1479.
52. **Schultz NA, Andersen KK, Roslind A, Willenbrock H, Wojdemann M, Johansen JS.** 2012. Prognostic microRNAs in cancer tissue from patients operated for pancreatic cancer—five microRNAs in a prognostic index. World J. Surg. **36:**2699–2707.
53. **Schultz NA, Werner J, Willenbrock H, Roslind A, Giese N, Horn T, Wojdemann M, Johansen JS.** 2012. MicroRNA expression profiles associated with pancreatic adenocarcinoma and ampullary adenocarcinoma. Mod. Pathol. **25:**1609–1622.
54. **Takahashi M, Cuatrecasas M, Balaguer F, Hur K, Toiyama Y, Castells A, Boland CR, Goel A.** 2012. The clinical significance of MiR-148a as a predictive biomarker in patients with advanced colorectal cancer. PLoS One **7:**e46684. doi:10.1371/journal.pone.0046684.
55. **Xu X, Fan Z, Kang L, Han J, Jiang C, Zheng X, Zhu Z, Jiao H, Lin J, Jiang K, Ding L, Zhang H, Cheng L, Fu H, Song Y, Jiang Y, Liu J, Wang R, Du N, Ye Q.** 2013. Hepatitis B virus X protein represses miRNA-148a to enhance tumorigenesis. J. Clin. Invest. **123:**630–645.
56. **Li J, Song Y, Wang Y, Luo J, Yu W.** 2013. MicroRNA-148a suppresses epithelial-to-mesenchymal transition by targeting ROCK1 in non-small cell lung cancer cells. Mol. Cell Biochem. **380:**277–282.